IEEE Access
Multidisciplinary | Rapid Review | Open Access Journal

Received March 31, 2022, accepted May 9, 2022, date of publication May 12, 2022, date of current version May 23, 2022.

Digital Object Identifier 10.1109/ACCESS.2022.3174601

Deviation From Model of Normal Aging in Alzheimer's Disease: Application of Deep Learning to Structural MRI Data and Cognitive Tests

TETIANA HABUZA[1,2], NAZAR ZAKI[1,2], ELFADIL A. MOHAMED[3], AND YAUHEN STATSENKO[4,5]

[1]Department of Computer Science and Software Engineering, College of Information Technology, United Arab Emirates University, Al Ain, United Arab Emirates
[2]Big Data Analytics Center (BIDAC), United Arab Emirates University, Al Ain, United Arab Emirates
[3]Artificial Intelligence Research Center (AIRC), College of Information Technology, Ajman University, Ajman, United Arab Emirates
[4]Radiology Department, College of Medicine and Health Sciences, United Arab Emirates University, Al Ain, United Arab Emirates
[5]Abu Dhabi Precision Medicine Virtual Research Institute (AD PM VRI), United Arab Emirates University, Al Ain, United Arab Emirates

Corresponding authors: Tetiana Habuza (201890064@uaeu.ac.ae) and Nazar Zaki (nzaki@uaeu.ac.ae)

This work was supported in part by the Alzheimer's Disease Neuroimaging Initiative (ADNI), National Institutes of Health, under Grant U01 AG024904; and in part by the Department of Defense (DOD), ADNI, under Award W81XWH-12-2-0012.

This work involved human subjects or animals in its research. Approval of all ethical and experimental procedures and protocols was granted by the Institutional Review Board, also known as an Independent Ethics Committee, under an ICMJE-approved registry, and performed in line with the Institutional and/or National Research Committee and the 1964 Helsinki Declaration and its later amendments or comparable ethical standards.

ABSTRACT **Background.** Psychophysiological and cognitive tests as well as other functional studies can detect pre-symptomatic stages of dementia. When assembled with structural data, cognitive tests diagnose NDs more reliably thus becoming a multimodal diagnostic tool. **Objective.** Our main goal is to improve screening for dementia by studying an association between the brain structure and its function. Hypothetically, the brain structure-function association has features specific for either disease-related cognitive deterioration or normal neurocognitive slowing while aging. **Materials and methods.** We studied a total number of 287 cognitively normal cases, 646 of mild cognitive impairment, and 369 of Alzheimer's disease. To work out a new marker of neurodegeneration, we created a convolutional neural network-based regression model and predicted the cognitive status of the cognitively preserved examinee from the brain MRI data. This was a model of normal aging. A big deviation from the model suggests a high risk of accelerated cognitive decline. **Results.** The deviation from the model of normal aging can accurately distinguish cognitively normal subjects from MCI patients (AUC = 0.9957). We also achieved creditable performance in the MCI-versus-AD classification (AUC = 0.9793). We identified a considerable difference in the MMSE test between A-positive and A-negative demented individuals according to ATN-criteria (6.27±1.82 vs 5.32±1.9; $p < 0.05$). **Conclusion.** The deviation from the model of normal aging can be potentially used as a marker of dementia and as a tool for differentiating Alzheimer's disease from non-Alzheimer's dementia. To find and justify a reliable threshold levels, further research is required.

INDEX TERMS Error of cognitive score prediction, biomarker, Alzheimer's disease, neuroimaging, convolutional neural network, deep learning, cognitive decline, dementia, aging.

ABBREVIATIONS

AD	Alzheimer's Disease.
ADAS	Alzheimer's Disease Assessment Scale.
ADNI	Alzheimer's Disease Neuroimaging Initiative.
AUC	Area Under the Curve.
BAC	Balanced Accuracy.
CDR	Clinical Dementia Rating.
CN	Cognitively Normal (Healthy Subject).
CNN	Convolutional Neural Network.
CT	Computed Tomography.
DMNA	Deviation from the Model of Normal Aging.
CSF	Cerebrospinal Fluid.
DL	Deep Learning.

The associate editor coordinating the review of this manuscript and approving it for publication was Yongming Li.

DSST	Digit Symbol Substitution Test.
MAE	Mean Absolute Error.
MCI	Mild Cognitive Impairment.
MMSE	Mini Mental State Examination.
ML	Machine Learning.
ND	Neurodegenerative disorder.
RAVLT	Rey Auditory-Verbal Learning Test.
ROC	Receiver Operating Characteristic Curve.
SFA	Structural-Functional Association.
TIV	Total Intracranial Volume.
TMT	Trail Making Test.

I. INTRODUCTION

A typical topic of studies in cognitive neuroscience is distinguishing between normal and accelerated aging manifesting itself with dementia. The primary goal is to explain operation of the human mind in the healthy condition and in pathology [1]. There are different ways to perform studies on cognition. The model-based cognitive neuroscience approach is the most commonly used routine. The models predict brain measures from some parameters and provide a potential explanation of brain functioning [2]. Depending on the study issues, researchers use symbolic, neural, connectionist, dynamical and other models. The conceptual framework selected for the study influences the issue of the study, the research questions we address, the experiments we perform, and the ways in which we interpret the results [3]. We intend to improve diagnostics of cognitive disorders and focus on the difference between the brain structure and function in normal and accelerated aging. Multimodal techniques for diagnosis and prognosis of Alzheimer's disease (AD) deserve particular attention as they are more sensitive and promote screening and early management strategies [4]. To use the advances of multimodal diagnostics, we resort to models of structure-function association (SFA). These models accumulate information from both structural and functional findings, which makes them more specific for norm or pathology.

Dementia is a disturbance of higher mental functions, such as reasoning, planning, judging and memorizing. The most common reason for dementia is Alzheimer's disease (AD). Currently, 57 million people worldwide suffer from dementia. This number is predicted to triple by 2050 and reach 152 million cases [5]. The reason for this exponential increment in dementia is aging of society which raises the incidence of neurodegenerative diseases (NDs). Diagnostics of NDs is challenging since neither structural signs nor functional tests are sensitive enough and specific. There is a big list of unresolved issues to cover. First, there is no reliable tool to predict whether the pre-dementia will progress. *Second*, it is impossible to perform the differential diagnostics of exact neurodegenerative diseases (ND) with non-invasive tests. For instance, the early differentiation between mild cognitive impairment (MCI) due to AD and MCI caused by other ND conditions is particularly challenging in clinical settings.

To improve the current situation, we propose a combined analysis of structural and functional data with machine learning (ML) [6]. The strengths and limitations of brain structural and functional assessment are briefly discussed below. As seen from the references, there is no agreement between researchers on which non-invasive diagnostic modality is more promising for screening purposes. We chose to focus on multimodal diagnostics to benefit from both types of data.

A. FUNCTIONAL TESTS FOR COGNITIVE ASSESSMENT

Physicians can use functional tests to improve early diagnostics of NDs. However, there are some clear disadvantages of the tests: they are time-consuming; they require a special testing environment to keep the subject focused. Besides these, their interpretation is challenging as there is no understanding of the pathophysiological mechanisms underlying cognitive decline, whose structural bases are not studied well [7]. At the same time, psychophysiological, cognitive tests and evoked potentials studies can detect purely pre-symptomatic stages of dementia. Many models of developing dementia include cognitive test scores as predictors [8]. The most commonly used cognitive tests are the Mini-Mental State Examination (MMSE) [9], Rey Auditory-Verbal Learning Test (RAVLT) [10], Alzheimer's Disease Assessment Scale cognitive subscale (ADAS-cog) [11], Digit Symbol Substitution Test (DSST) [12], Trail Making Test (TMT) [13], Clinical Dementia Rating (CDR) [14], Logical Memory Tests (LMT), Immediate and Delayed Recall Test [15].

When assembled with structural data, cognitive tests indentify NDs more reliably thus becoming a multimodal diagnostic tool [16], [17]. Few studies focused on the prediction of the cognitive status from brain structural images (see Table 1). Some authors predicted MMSE scores from resting state functional MRI of patients with AD [18]. While others calculated MMSE, ADAS-cog, and CDR scores from structural MRI [19]. The prediction of the results of the tests that reflect a lower number of cognitive domains (e.g., RAVLT) was less accurate than of the tests covering a larger set of the domains (ADAS or MMSE). Another research team predicted MMSE and ADAS-cog scores with the model that integrated spatial-temporal features of the brain received from MRI findings [20]. Recent studies provided an insight into neurophysiological and morphological characteristics of the brain in patients with dementia [16]–[20]. However, the clinical utility of the proposed models remains limited.

B. BRAIN MORPHOLOGY STUDIES WITH MRI

The current study is dedicated to automatic analysis of MRI findings which can be used for screening. Structural MRI is a valid marker of the late stages of AD [21], but at an early stage it is not particularly revealing about the difference of the brain structural change in normal and accelerated aging. For this reason, some authors believe that a reliable means of identifying individuals at risk of AD should derive from electrophysiological diagnostics (e.g., event-related potentials) [8], [22].

Contrarily, there is evidence that neuropathological changes can be detected with neuroimaging much earlier than cognitive decline becomes apparent [23]. Structural MRI examinations reveal that the extent of age-related brain change varies markedly across individuals [24]. Studies on brain functioning bare inconsistencies in both the onset and the rate of episodic memory loss among the elderly. Inherited and lifestyle factors may account for these discrepancies. There is no direct link between structural and functional impairment. Researchers try to discover the structure-function relationship in the brain with advanced methods of neuroimaging [7], [25]. They show the importance of visual rating scales, volumetric assessment, and structured reporting.

A few brain regions are vulnerable to atrophy in NDs: hippocampus, amygdala, entorhinal cortex, fusiform gyrus, putamen, medial temporal lobe, etc. The aforementioned structures are neural centers responsible for learning, memory, navigation, processing information, emotions, behavior and time perception. Some authors study the brain at the macrostructural level. With MRI they assess the enlargement of gray matter, white matter (WM), ventricles, and accumulation of WM lesions - hyperintensitive areas in the T2-weighted sequence [26], [27]. Other researches focus on microstructural effects of NDs, e.g. neuronal death, accumulation of β-amyloid and τ-protein in hippocampus, etc. [28], [29]. Macrostructural characteristics of the brain (tissue volumes) can be identified with MRI and used for screening for NDs. Microstructural features (tissue organization) serve as golden standards of diagnostics.

C. MACHINE LEARNING METHODS

Processing biomedical images with ML techniques is a field of ongoing studies [30]. It has been already shown that an association between structural and functional changes of the brain can be studied with ML [6]. Numerous conventional ML and deep learning (DL) methods were proposed to discriminate AD patients from cognitively preserved people with structural MRI data [31]. For instance, Altaf *et al.* used a combination of textures (i.e., gray level co-occurrence matrix) and clinical features (i.e., MMSE) to predict the final diagnosis [32]. Ahmed *et al.* resorted to the bag-of-visual-words approach to generate a unique signature of an individual brain from hippocampus and posterior cingulate cortex [33]. Khedher *et al.* analyzed tissue-segmented MRI (i.e., white and gray matter images) to diagnose AD at an early stage [34]. Other authors used slices or 2D patches extracted from T1-weighted MRI as predictors in designed 2D-convolutional neural network (CNN) models [35]–[38]. Recently, 3D patches extracted from MRI were used to segregate healthy individuals from patients with MCI or AD [39]. The authors extracted voxels corresponding to hippocampus and used them as an input to 3DCNN classification model [40]. 3D images of the whole brain also served as an input to 3D subject-level CNNs [36], [41]–[47]. Qiao *et al.* used a 3DCNN with sharing weights to extract the features from MRI, followed by multiple sub-networks which transformed the MMSE regression models into a series of binary classification models [46]. All the methods discussed are summarized in Table 1. We presume that new findings on the brain structure-function association may foster further research on earlier detection and treatment of NDs. Multimodal diagnostics that we develop with ML accumulates the advantages of morphological and functional findings.

D. OBJECTIVE AND SUB-OBJECTIVES

Our main goal is to improve screening for dementia by studying an association between the brain structure and its function. *Hypothetically*, the brain SFA has features specific for either disease-related cognitive deterioration or normal neurocognitive slowing in aging. To address this objective, we formulate the following tasks:

- Conduct an exploratory analysis of structural and functional change in cognitively preserved population and in subjects diagnosed with MCI or dementia.
- Propose a reliable marker of disease-related cognitive decline.
- Justify the proposed marker as a screening tool for MCI and dementia.
- Test if the proposed marker can prognosticate the conversion of pre-dementia to dementia and differentiate cognitive decline due to AD from other NDs.

II. MATERIALS AND METHODS

A. DATASET

The data used in this study were obtained from the Alzheimer's Disease Neuroimaging Initiative (ADNI) database [62]. ADNI1 includes 400 subjects diagnosed with MCI, 200 subjects with early AD, and 200 elderly control subjects in the 55-90 age range [63]. See inclusion and exclusion criteria at [64]. For more information about ADNI datasets, visit the link https://adni.loni.usc.edu/. In this study, we acquired MRI and clinical information on all the cases collected to ADNI1 dataset in a cross-sectional and longitudinal study design. This provided us with a total number of 1,337 study cases from 800 subjects. We excluded 35 cases from our study because of a failure of FreeSurfer to segment the brain MRI. For the remaining 1,302 cases (CN/MCI/AD: 22.04% /49.62% /28.34%; male/female: 59.91%/40.09%), we collected the following information:

- Clinical data on the final diagnosis.
- Demographic data (i.e., age, gender, ethnicity).
- Morphometric data (i.e., volumes of brain areas mostly affected by ND).
- Results of cognitive assessment with MMSE, RAVLT, TMT (part B), DSST, ADAS-cog tests.
- Pre-processed T1-weighted MRI files.

B. PROPOSED FRAMEWORK

Figure 2 shows the general idea of proposed SFA model and Figure 3 illustrates the proposed framework.

TABLE 1. Recent papers related to diagnostics of MCI and AD.

Reference	Year	Dataset	Image modality	Training dataset	Prediction		Cognitive tests					
					Diagnosis	SFA	ADAS	MMSE	RAVLT	CDR	DSST	TMT
Stonnington et al. [19]	2010	ADNI + in-house	MRI	CN+AD		✓	✓	✓	✓	✓		
Liu et al. [48]	2013	ADNI	MRI	CN+MCI+AD	✓							
Gupta et al. [35]	2013	ADNI	MRI	CN+MCI+AD	✓							
Payan et al. [36]	2015	ADNI	MRI	CN+MCI+AD	✓							
Ahmed et al. [33]	2015	ADNI	MRI	CN+MCI+AD	✓							
Sorensen et al. [49]	2015	ADNI + AIBL [50] + Metropolit [51]	MRI	CN+MCI+AD	✓	✓		✓				
Li et al. [52]	2015	ADNI	MRI	CN+MCI+AD	✓		✓	✓				
Khedher et al. [34]	2015	ADNI	MRI	CN+MCI+AD	✓							
Hosseini-Asl et al. [53]	2016	ADNI	MRI	CN+MCI+AD	✓							
Suk et al. [54]	2016	ADNI	MRI	CN+MCI+AD	✓							
Gao et al. [55]	2017	Navy General Hospital (China)	CT	CN+MCI+AD	✓							
Zhang et al. [56]	2017	ADNI	MRI	CN+MCI+AD	✓							
Korolev et al. [41]	2017	ADNI	MRI	CN+MCI+AD	✓							
Cui et al. [40]	2018	ADNI	MRI	CN+MCI+AD	✓							
Billones et al. [44]	2017	ADNI	MRI	CN+MCI+AD	✓							
Liu et al. [57]	2018	ADNI	MRI + PET	CN+MCI+AD	✓							
Altaf et al. [32]	2018	ADNI	MRI + PET	CN+MCI+AD	✓							
Lee et al. [37]	2019	ADNI	MRI	CN+MCI+AD	✓							
Lahrimi et al. [17]	2019	ADNI	MRI + tests	CN+AD	✓		✓	✓				
Basaia et al. [42]	2019	ADNI + in-house	MRI	CN+MCI+AD	✓							
Lei et al. [20]	2019	ADNI	MRI	CN+MCI+AD		✓	✓	✓				
Fang et al. [58]	2019	ADNI	MRI	CN+MCI+AD	✓							
Liu et al. [39]	2020	ADNI	MRI	CN+MCI+AD	✓							
Wang et al. [43]	2020	ADNI	MRI	CN+MCI+AD	✓							
Duc et al. [18]	2020	In-house	rs-fMRI	CN+AD	✓	✓		✓				
Zhang et al. [59]	2021	ADNI	MRI	CN+MCI+AD	✓							
Sathiyamoorthi et al. [60]	2021	ADNI	MRI	CC+MCI+AD	✓							
Qiu et al. [61]	2022	ADNI+OASIS	MRI	CN+MCI+AD	✓							
Soliman et al. [45]	2022	ADNI	MRI	CN+AD	✓							
Qiao et al. [46]	2022	ADNI	MRI	CN+MCI+AD		✓		✓				
Gao et al. [47]	2022	ADNI	MRI	CN+AD	✓							
Proposed		ADNI	MRI	CN	✓	✓	✓	✓	✓		✓	✓

CDR - clinical dementia rating score [14]

The first objective was to conduct a comparative analysis of the brain structure and function in CN subjects, MCI and AD groups. We evaluated the separability of the three groups with non-parametric statistical methods, i.e. Kruskal-Wallis test for the continuous features and the Chi-square test for the quantitative ones.

The second objective was to propose a new marker of accelerated cognitive decline. In line with the hypothesis of the study, we proposed to predict the cognitive status of the cognitively preserved examinee from the brain MRI data and worked out the SFA model. Then we applied the SFA model to the findings of the study group. When the findings of a scanned individual did not fit the standard SFA model, accelerated aging was suspected. We calculated the deviation from the model of normal aging (DMNA) as the error of cognitive score prediction (see Equation 1).

$$DMNA = y_{predicted} - y_{actual} \tag{1}$$

where y is a result of the cognitive test.

Modeling cognitive performance from MRI is a complex problem. To reduce its computational complexity, we transformed MRI images into two-dimensional data (see subsection II-C). Then we designed CNN model and trained it on images of CN individuals. To generalize the model to a true rate error, we utilized the five-fold cross-validation technique.

As an input, we used the pre-processed MRI data ($D^{(CN)}_{axial}$, $D^{(CN)}_{coronal}$,$D^{(CN)}_{sagittal}$). The output variables were the results of the following cognitive tests: MMSE, RAVLT, TMT (part B), DSST, ADAS-cog. After the prediction of cognitive performance we calculated DMNA (see Equation 1).

1) THE THIRD OBJECTIVE WAS TO JUSTIFY THE RELIABILITY OF DMNA)

It was a three-fold task. First, we employed non-parametric statistical tests to compare DMNA values of the CN group with MCI and AD patients. Second, we created ML models that distinguish the following study cohorts by DMNA values: CN people from patients with MCI, and patients with MCI from those with AD. The models were trained with the ten-fold cross-validation technique. Finally, we evaluated their performance. The performance of the regression models

was expressed as mean absolute error (MAE). The accuracy of the classification model was assessed with Sensitivity, Specificity, F-measure, ROC, AUC, Accuracy, and Balanced Accuracy.

2) THE FOURTH OBJECTIVE WAS TWO-FOLD

In the first part of sub-objective four, we tested if the proposed marker can prognosticate the conversion of pre-dementia to dementia. To find the cases of stable and progressive MCI, we did an exhaustive search in all longitudinal studies: ADNI1, ADNI2, ADNI-GO, ADNI3. Then, we built the conventional ML model segregating the cases according to stability/progression. We used DMNA in MMSE and ADAS-cog as more reliable predictors because the tests covered the global cognitive functioning. To compare the distribution of DMNA in two groups, we applied the non-parametric Kruskal-Wallis test. We also assessed sensitivity and specificity of the model classifying MCI cases into stable and progressive ones.

The second part of sub-objective four was to check if DMNA could differentiate cognitive decline due to AD from other NDs. To address the research question, we resorted to ATN criteria [65] and adopted a two-step analysis. Firstly, we dichotomized each biomarker category as either normal (-) or abnormal (+) with the following cutoff thresholds. A case was considered as A- if the CSF concentration of beta-amyloid was higher than 81/ml [66], [67], T- if the level of p-tau was less than 56 pg/ml [66], [68], and N- if FDG-PET uptake was larger than 1.21 [69]. Secondly, we classified all the cases with MCI and dementia into groups and calculated mean values of DMNA for them (see Table 6). Finally, we identified the difference in DMNA between demented individuals with Alzheimer's continuum (A+) and those with either normal AD biomarkers or non-AD pathologic change (A–).

C. DATA PRE-PROCESSING

All the retrieved images passed through grad-warping and intensity correction and were scaled to gradient drift with the phantom data (for more details, see [63]). The pre-processed T1 weighted structural MRI images were downloaded in NIFTI format. We also retrieved the corresponding clinical data from the dataset. Then the images were registered to an MNI152 space with FLIRT tool from FSL package [70]. As brains differ in size and shape, each brain image was translated into a common reference space (normalized) to ensure consistency of orientation. To correct low-frequency intensity non-uniformity, we used N4 bias field correction algorithm [71]. Then we normalized the voxel intensities by scaling them to the standard normal distribution parameters. To enhance the predictive performance, we extracted the brain parenchyma with Brain Extraction Tool (BET) from FSL package [70].

One of the major challenges of studies on MRI is a high dimensionality of data [72]. We used the following approach to reduce it. An MRI image was defined as

$$I = \{(v_x, v_y, v_z) : x = \overline{1, X}, y = \overline{1, Y}, z = \overline{1, Z}\}, \quad (2)$$

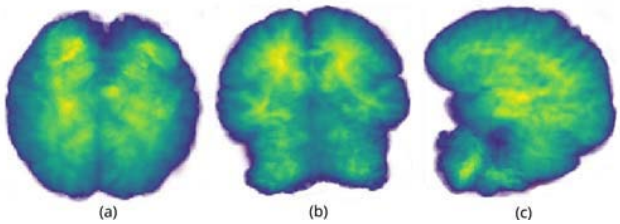

FIGURE 1. Skull-stripped images averaged along axial (a), coronal (b), and sagittal (c) axes.

where X,Y,Z were the dimensions of the MRI scan in axes x, y and z. Then the j^{th} sagittal, coronal or axial slice s of the I image could be defined as:

$$\begin{aligned} s^{(j)}_{sagittal} &= (j, v_y, v_z), \\ s^{(j)}_{coronal} &= (v_x, j, v_z), \\ s^{(j)}_{axial} &= (v_x, v_y, j) \end{aligned} \quad (3)$$

The corresponding averaged images were generated as follows:

$$I_{sagittal} = \frac{1}{X}\sum_{i=1}^{X} s^{(i)}_{sagittal}$$

$$I_{coronal} = \frac{1}{Y}\sum_{i=1}^{Y} s^{(i)}_{coronal}$$

$$I_{axial} = \frac{1}{Z}\sum_{i=1}^{Z} s^{(i)}_{axial}$$

In this way, we averaged voxel intensities along the sagittal, coronal and axial axes and created two-dimensional datasets D_{axial}, $D_{sagittal}$, and $D_{coronal}$:

$$\begin{aligned} D_{axial} &= \{I^1_{axial}, I^2_{axial}, \ldots, I^N_{axial}\} \\ D_{sagittal} &= \{I^1_{sagittal}, I^2_{sagittal}, \ldots, I^N_{sagittal}\} \\ D_{coronal} &= \{I^1_{coronal}, I^2_{coronal}, \ldots, I^N_{coronal}\} \end{aligned}$$

Then, we removed the background by cropping the image to the size of the brain mask. We down-sampled brain images with nearest-neighbor interpolation to the size of 150 by 150 pixels, normalized them within the range of 0 to 1, and stored in JPEG format as shown in Figure 1. To unify the pre-processing workflow, we used Nipype which is an open-source community-developed initiative under the umbrella of NiPy [73]. To automate the deployment of the applications within the software containers, we installed Neurodocker which wraps up the aforementioned software in a complete file system.

D. STATISTICAL ANALYSIS AND MACHINE LEARNING

We calculated volumes of WM hyperintensities and the following structures: interventricular CSF, hippocampus, putamen, caudate nucleus, amygdala, WM, enthorinal cortex, fusiform gyrus, middle temporal lobe, gray matter, its cortex and total intracranial volume. Subcortical and cortical

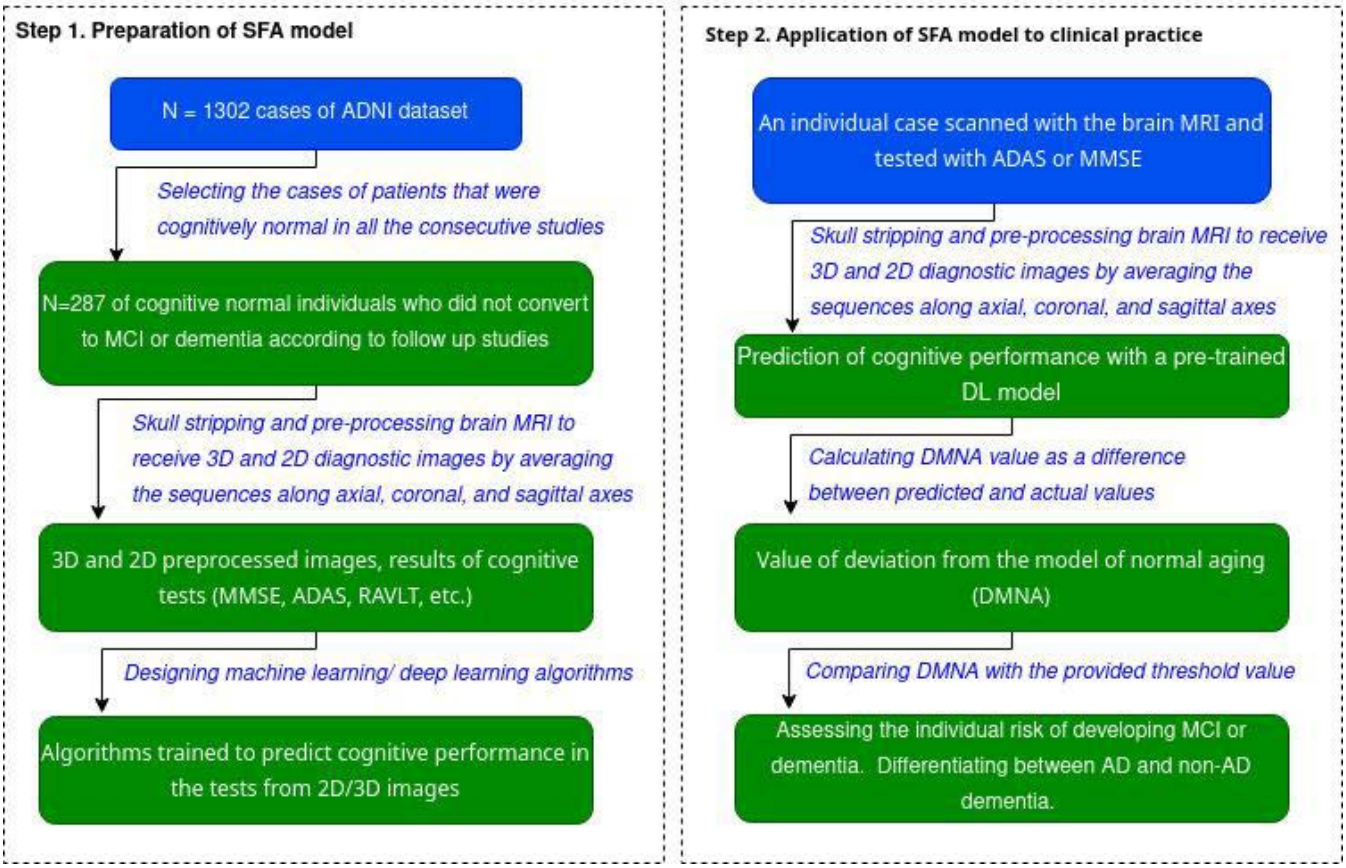

FIGURE 2. **Preparation and application of the proposed SFA model to clinical practice.**

parcellation volumes were computed with FreeSurfer 7.1.0 software [74]. We resorted to Desikan/Killiany atlas as a reference. All features were expressed as percentage to the total intracranial volume and used as an input to the ML model predicting the cognitive scores.

The functional data were presented with the results of the following cognitive tests: MMSE, DSST, TMT (part B), ADAS-cog ($ADAS_{Q4}$, $ADAS_{11}$, and $ADAS_{13}$) and RAVLT ($RAVLT_{immediate}$, $RAVLT_{learning}$, and $RAVLT_{forgetting}$) [62]. The associations between CSF% and performance in ADAS-cog and RAVLT were stronger for ADAS-13 and $RAVLT_{immediate}$ compared to the other scores in these test. For this reason we used ADAS-13 and $RAVLT_{immediate}$ for further analysis (see section III-A).

We started the statistical analysis by looking at the relationship among the attributes. The associations of the cognitive test scores with age, functional and structural data in healthy cohort and subjects diagnosed with MCI and AD were assessed with Pearson's correlation coefficient. Then, we inspected the attributes for Gaussianity. Shapiro-Wilk test revealed the non-normal distribution of all the attributes. Therefore, we utilized non-parametric statistical tests for further analysis. To check if the data from the studied groups (CN, MCI, AD) came from a common distribution we used Kruskal-Wallis test with the continuous features and the Chi-square test with the quantitative ones. The results were expressed as *IQR*, *mean* $\pm$ *std* or the number of cases, and their percentage in the observed group.

To predict cognitive scores from the structural data, we designed a CNN model. The proposed CNN regression model consisted of six convolution layers followed by two fully connected dense layers. The model was regularized with L2 penalty and $\alpha = 0.0001$. We used RMSProp optimizer and trained the network for 200 epochs or until convergence. To optimize a learning rate hyperparameter, we monitored the validation loss during the training process. When the metric stopped improving for 10 continuous epochs, we multiplied the learning rate value by 0.2. To optimize the training time, we also monitored the validation loss. If it did not decrease for 20 continuous epochs, we terminated the training process. 20% of the training data was used for validation purposes. The model was trained on the CN cohort in the five-fold cross-validation technique. There were several arguments in favor of the necessity to train models of SFA on non-demented cases exceptionally. As the model reflected the brain SFA for the healthy controls, it could be used as a reference norm. If trained on a mixed cohort of healthy individuals and patients, the model would fail to identify the patients out of the reference range and would lose its diagnostic value. The

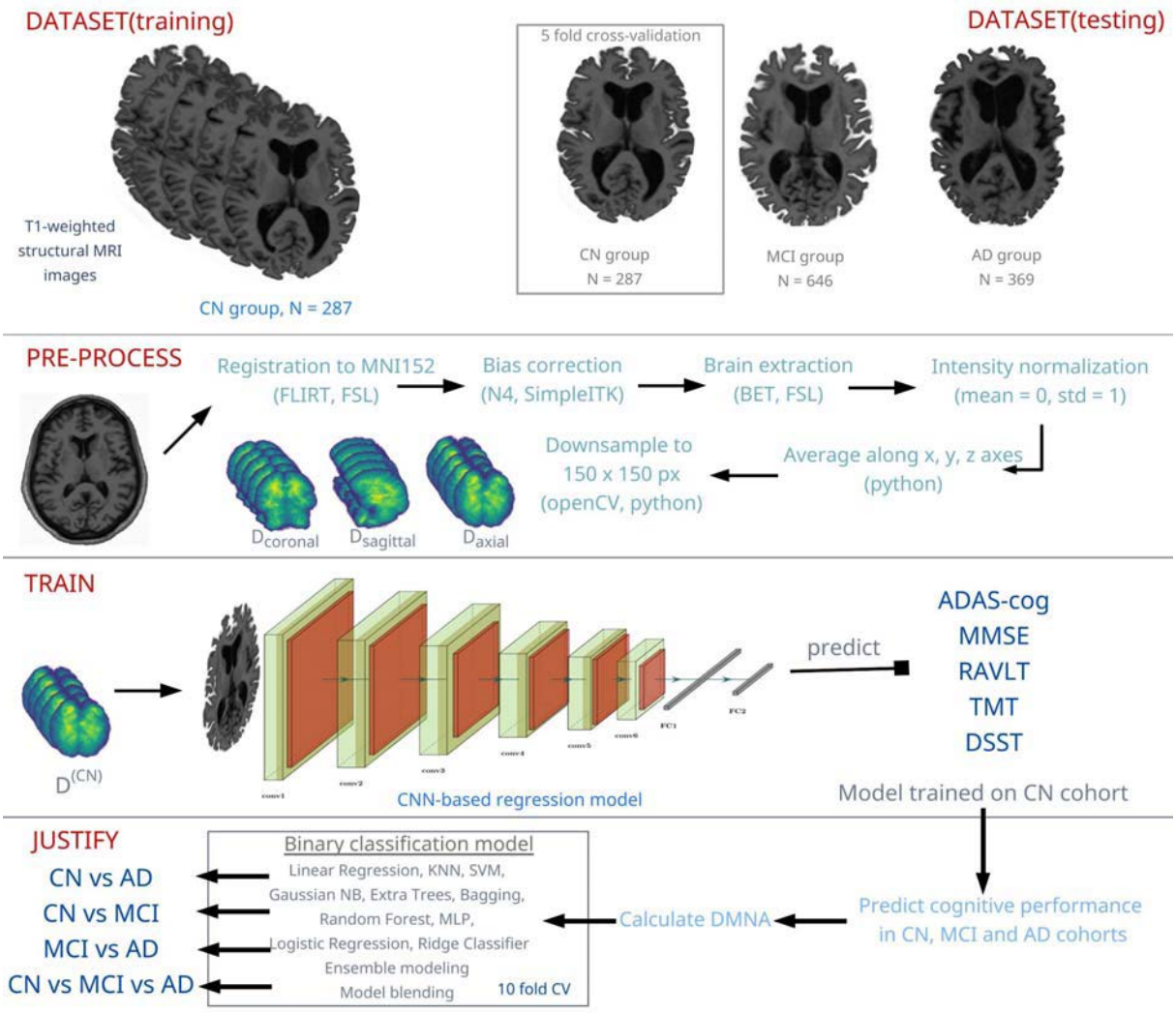

FIGURE 3. Pipeline of proposed framework.

trained model from the last fold was tested on MCI and AD groups.

For each case we had 2D images obtained by averaging brain MRI in three planes: axial (A), coronal (B), and sagittal (C). We could use them either separately or in combination. For the combined approach we used two options: data and model blending. The first one was fusing predictions, which was an ensemble estimator or voting regressor that averaged model outcomes. The second method was model blending. We trained the linear regression (LR) model on the outcomes of three CNN models trained on axial, coronal, and sagittal averaged images. The outcomes of the predictive algorithm were the results of mental status tests such as MMSE, RAVLT, DSST, ADAS-cog, and TMT (Part B).

We compared the distribution of the DMNA absolute values in the healthy population and patients with MCI and Dementia. We also calculated 95% confidence intervals for DMNA values with the t-test. To control the familywise error rate related to multiple comparisons we employed Bonferroni correction. All statistical tests were performed in Python v. 3.6.9 with SciPy v. 1.16.4 library [75].

The experimental work was performed with the help of Linux Ubuntu 18.04 Nvidia DGX-1 deep learning server with 40 CPU cores and 8x NVIDIA Tesla V100 GPU with 32 GB memory each, accessed with a web-based multi-user concurrent job scheduling system [76]. The tensorflow-gpu v.2.3.1 library was utilized to implement the proposed solution.

III. RESULTS

A. DEMOGRAPHIC, FUNCTIONAL, AND STRUCTURAL DATA IN STUDIED COHORTS

The structural data are presented in terms of percentage of the volume of a specific brain area to the total intracranial volume. There are significant differences among the studied cohorts in the structures most vulnerable to change in ND (see Table 2). The data reveal shrinkage of the brain parts (hippocampus, entorhinal cortex, fusiform gyrus, medial

TABLE 2. Demographics, cognitive performance and volumes of brain parts in studied groups.

	Total N= 1302	CN 287(22.04%)	MCI 646(49.62%)	Dementia 369(28.34%)	p-value
Age	75.74[71.7-80.7]	76.62±5.62	75.25±7.16	75.93±7.37	0.0933785
Gender					**4.19707e-06**
Female	522(40.09%)	134(46.69%)	215(33.28%)	173(46.88%)	
Male	780(59.91%)	153(53.31%)	431(66.72%)	196(53.12%)	
Education, years	15.58[13.0-18.0]	16.13±2.91	15.76±2.99	14.85±3.21*	**9.08991e-08**
Ethnicity					0.198438
White	1210(92.93%)	261(90.94%)	603(93.34%)	346(93.77%)	
Black	60(4.61%)	21(7.32%)	22(3.41%)	17(4.61%)	
Asian	30(2.3%)	5(1.74%)	19(2.94%)	6(1.63%)	
Indian/Alaskan	1(0.08%)	0(0.0%)	1(0.15%)	0(0.0%)	
More than one	1(0.08%)	0(0.0%)	1(0.15%)	0(0.0%)	
Marital status					**4.1773e-08**
Married	1035(79.49%)	196(68.29%)	532(82.35%)	307(83.2%)	
Never married	31(2.38%)	13(4.53%)	6(0.93%)	12(3.25%)	
Divorced	79(6.07%)	21(7.32%)	42(6.5%)	16(4.34%)	
Widowed	154(11.83%)	54(18.82%)	66(10.22%)	34(9.21%)	
Unknown	3(0.23%)	3(1.05%)	0(0.0%)	0(0.0%)	
Cognitive tests					
ADAS-cog	19.87[11.67-26.33]	8.73±4.14	18.82±6.6	30.37±8.97	**2.2404e-165**
MMSE	26.18[24.0-29.0]	29.06±1.09	26.91±2.2	22.66±3.03	**2.1560e-155**
RAVLT	30.44[23.0-37.0]	43.2±9.76	29.79±8.86	21.67±7.77	**3.7071e-120**
DSST	36.24[27.0-45.0]	46.77±11.06	37.37±11.1	26.05±12.41	**2.72808e-83**
TMT(part B)	138.13[75.0-187.0]	85.03±43.18	128.48±72.56	200.96±88.57	**2.20487e-73**
Morphometry					
Ventricles	2.93[1.82-3.67]	2.52±3.73	2.86±1.35	3.37±1.46	**1.13635e-23**
Hippocampus	0.41[0.35-0.46]	0.47±0.06	0.4±0.07	0.36±0.07	**1.93988e-65**
Putamen	0.53[0.48-0.57]	0.55±0.06	0.52±0.06	0.51±0.08	**1.54782e-17**
Amygdala	0.15[0.13-0.17]	0.18±0.02	0.15±0.03	0.14±0.03	**8.82095e-64**
WM lesions	0.41[0.17-0.47]	0.32±0.31	0.38±0.38	0.54±0.5	**2.23640e-17**
Entorhinal cortex	0.21[0.17-0.25]	0.25±0.04	0.21±0.05	0.18±0.05	**2.14294e-58**
Fusiform gyrus	1.03[0.93-1.13]	1.1±0.13	1.04±0.14	0.95±0.14	**2.06811e-30**
Middle temporal lobe	1.18[1.06-1.29]	1.28±0.13	1.18±0.16	1.07±0.15	**8.55332e-48**
Whole brain	63.19[60.16-65.83]	65.51±4.54	63.29±3.92	61.21±3.89	**1.84928e-36**

P-value is marked in bold if difference among groups is statistically significant ($p < 0.05$).
Structural features are reported in % to TIV. Statistical data are expressed as IQR, $Mean \pm SD$, or the absolute number of cases and their percentage in studied cohort.

TABLE 3. Performance of models trained on cognitively preserved population and tested on three different cohorts(MAE).

Data	Method	MMSE			ADAS-cog			RAVLT			TMT(part B)			DSST		
		CN	MCI	AD	CN	MCI	AD	CN	MCI	AD	CN	MCI	AD	CN	MCI	AD
Axial(A)	CNN	1.12	2.54	6.54	5.74	10.54	21.95	8.74	14.41	21.4	44.39	109.44	183.62	9.5	12.39	20.8
Coronal (C)	CNN	1.09	2.5	**6.08**	3.69	12.51	24.19	8.4	**12.84**	**19.42**	47.09	114.97	189.33	9.06	**11.34**	**18.3**
Sagittal (S)	CNN	1.17	2.46	6.37	3.56	10.89	22.15	9.9	14.31	21.18	47.6	58.08	123.65	9.51	11.84	20.24
VR(C+S)	ensemble	1.13	2.48	6.23	3.63	11.7	23.17	9.15	13.58	20.3	47.34	86.52	156.49	9.28	11.59	19.27
VR(A+C)	ensemble	1.11	2.52	6.31	4.72	11.53	23.07	8.57	13.63	20.41	45.74	112.21	186.47	9.28	11.86	19.55
VR(A+S)	ensemble	1.15	2.5	6.45	4.65	10.72	22.05	9.32	14.36	21.29	46.0	83.76	153.64	9.51	12.11	20.52
VR(A+C+S)	ensemble	1.13	2.5	6.33	4.33	11.32	22.76	9.02	13.85	20.67	46.36	94.16	165.54	9.36	11.85	19.78
MB(A+C+S)	CNN+LR	**0.84**	**2.38**	6.46	**3.44**	**10.29**	**21.56**	**7.94**	14.63	21.78	**29.67**	**55.74**	**120.08**	**8.67**	11.93	21.26

A, S and C correspond to skull stripped images averaged along appropriate axis; VR - Voting Regression meta-estimator;
MB - Model Blending; LR - Linear Regression; RR - Ridge Regression.

temporal lobe) and enlargement of ventricles in accelerated aging. No significant differences in age among CN, MCI and AD groups was detected ($p = 0.1109$).

In the MCI cohort, the ADAS-cog score is negatively associated with the major part of the analyzed relative volumes. The exception is the relative volume of WM, CSF, WM lesion, and caudate nucleus. The association of performance in ADAS-cog with the relative volume of caudate nucleus is almost significant ($p = 0.061$). The portion of TIV occupied by WM lesions does not correlate with ADAS-cog scores in this group ($r = 0.03$; $p = 0.38$). WM lesions are a typical sign of brain aging. They result from chronic small vessel disease and can be seen well as foci or areas hypointensive on T1-weighted images and hyperintensive on T2-weighted images including FLAIR. There are different patterns of the emergence of the WM lesions in MCI and AD groups.

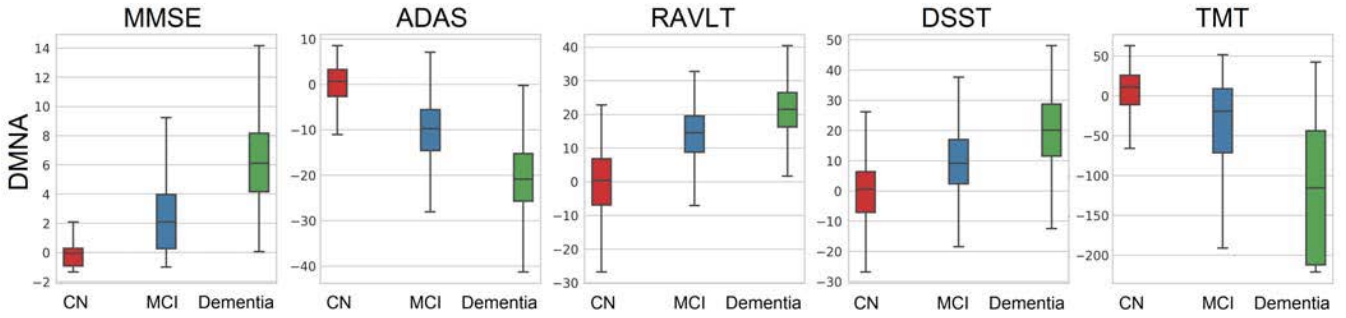

FIGURE 4. Distribution of deviation from model of normal aging among study cohorts.

TABLE 4. Mean absolute error of voting regression ensemble model trained on structural brain images averaged along axial, coronal and sagittal axes.

	CN group		MCI group		AD group		
	Mean±STD	95%CI	Mean±STD	95%CI	Mean±STD	95%CI	p-value
MMSE	0.84±0.73	[0.75 - 0.92]	2.38±2.08	[2.23 - 2.54]	6.46±3.04	[6.15 - 6.77]	**4.8422e-142**
ADAS-cog	3.44±2.42	[3.16 - 3.72]	10.29±6.15	[9.82 - 10.77]	21.56±8.94	[20.64 - 22.47]	**4.3343e-150**
RAVLT	7.94±5.86	[7.26 - 8.62]	14.63±7.21	[14.07 - 15.18]	21.78±7.84	[20.98 - 22.58]	**1.08195e-91**
TMT(part B)	29.67±31.42	[26.03 - 33.31]	55.74±62.73	[50.9 - 60.58]	120.08±79.28	[111.98 - 128.18	**8.91918e-53**
DSST	8.67±7.0	[7.86 - 9.48]	11.93±8.51	[11.27 - 12.58]	21.26±11.73	[20.06 - 22.45]	**3.51058e-54**

The functional data in ADNI1 are obtained with cognitive tests such as MMSE, ADAS-cog ($ADAS_{Q4}$, $ADAS_{11}$, $ADAS_{13}$), DSST, RAVLT ($RAVLT_{immediate}$, $RAVLT_{learning}$, $RAVLT_{forgetting}$), and TMT (part B) [62]. The association between the major marker of brain atrophy - CSF% - and performance in ADAS-cog tests is stronger for $ADAS_{13}$ ($r = 0.18$; $p < 0.05$) than for $ADAS_{Q4}$ ($r = 0.15$; $p < 0.05$) and $ADAS_{11}$ ($r = 0.15$; $p < 0.05$). This goes in line with a research which evidenced a more pronounced annual decline in $ADAS_{13}$ than in $ADAS_{11}$ in AD patients [77]. Similarly, the association of CSF% score with $RAVLT_{immediate}$ is stronger than with $RAVLT_{learning}$ and $RAVLT_{forgetting}$ scores ($r = -0.19$ vs -0.10 and 0.12; $p < 0.05$). Other authors also showed that the accuracy of the model predicting RAVLT scores from gray matter density is higher for $RAVLT_{immediate}$ score than for $RAVLT_{forgetting}$ [78]. Therefore, we used $ADAS_{13}$ and $RAVLT_{immediate}$ in this study. Figure 5 shows the associations of the test results with age and structural data.

SFA. ADAS-cog and MMSE are primary cognitive tests required in all recent Food and Drug Administration clinical drug trials for AD in the USA [79]. From our data, the results in ADAS-cog and RAVLT had the strongest association with the structural markers of brain atrophy in the CN group. For instance, the coefficient of correlation between hippocampal volume and $ADAS_{13}$ score was -0.18 in the CN cohort, -0.34 in patients with MCI, and -0.20 in the AD group. The same coefficient in $RAVLT_{immediate}$ was 0.13, 0.24, and 0.18 in the correspondent cohorts (see Figure 5).

B. PROPOSED MARKER OF DISEASE-RELATED COGNITIVE DECLINE

When applied to distinct cognitive test scores, the proposed CNN model shows the best prediction performance in the CN cohort (see Table 3). The worst performance was monitored in the AD group. Data-blending did not boost the performance considerably, i.e., there was no evident advantage in using several image reconstructions. In contrast to this, the model-blending approach showed the top accuracy. It allowed us to retrieve maximum data for assessing SFA (see Figure 4). The variability of the results in the studied cohorts is most apparent in ADAS-cog and MMSE tests and less evident in RAVLT, DSST, and TMT. The distribution of MAE differs significantly among the cohorts (see Table 4). This justifies that cognitively-normal people and patients with NDs have different SFA patterns, which can aid to diagnostics of MCI and AD.

TABLE 5. Threshold values of the DMNA markers in binary classification.

Cognitive test	CN vs MCI		MCI vs AD	
	Threshold	Accuracy	Threshold	Accuracy
MMSE	1.0298	0.7889	4.2011	0.9153
ADAS-cog	5.0856	0.9068	18.1063	0.9172
RAVLT	6.2389	0.7921	18.1036	0.7862
TMT(part B)	37.8308	0.8435	146.1889	0.8079
DSST	1.8726	0.7085	15.747	0.802

*Threshold values are expressed as absolute values of DMNA

C. JUSTIFICATION OF DMNA AS MARKER OF DEMENTIA

To determine a diagnosis from DMNA values, we employed nine conventional ML classifiers (SVM linear and non-linear, Gaussian NB, Extra Trees, Bagging, Random Forest, Logistic Regression, Ridge Regression, Neural Network). DMNA values were obtained from skull-stripped brain images averaged along the axial, coronal, and sagittal axes. The ML models were evaluated with the ROC AUC metric.

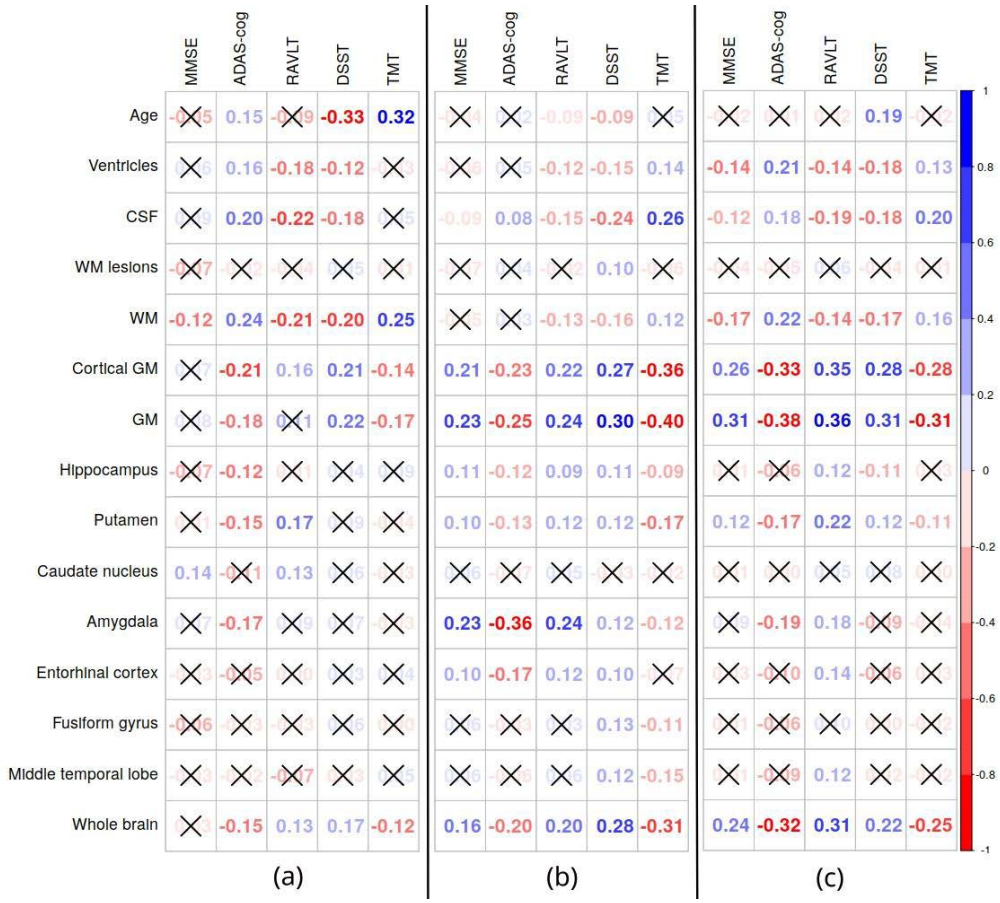

FIGURE 5. Associations of results in cognitive tests with age, functional and structural features in healthy cohort (a), patients with MCI (b) and AD (c). Association is reported in terms of Pearson's correlation coefficient. Cross-mark overlays non-significant relationships between features ($p > 0.05$).

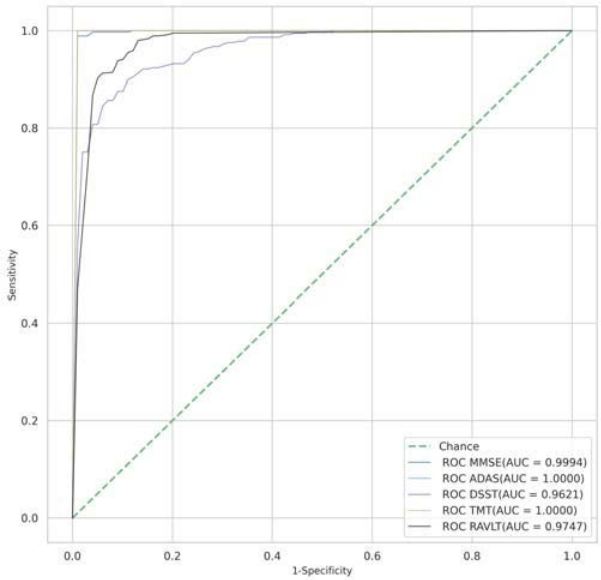

FIGURE 6. Performance of Random Forest model classifying cases into healthy and AD groups. DMNA values are input to the model.

Diagnosing from DMNA values was most accurate with Random Forest classifier jointly trained on DMNA MMSE and DMNA ADAS-cog (see Table 4, Figures 6 and 7). The performance of the CN-versus-AD classification model ($AUC = 1.0$) was comparable to the accuracy of state-of-the-art models trained on ADNI dataset (see Table 6). From the table, DMNA can accurately distinguish CN subjects from MCI patients ($AUC = 0.9957$). We also achieved creditable performance in the MCI-versus-AD classification ($AUC = 0.9793$). Therefore, DMNA can be potentially used as a marker of dementia and can help to identify the disease. Moreover, to use the proposed approach in clinics, we assessed the possible threshold values of DMNA markers. We undertook sequential values of DMNA and calculated the accuracy of the CN vs MCI and MCI vs AD classification. Table 5 lists the thresholds of DMNA markers in the binary classification models. The optimal performance is noted in the models based on ADAS-cog scores. These models allowed us to distinguish normal aging from MCI and the latter from AD with a high accuracy (above 90%).

D. PREDICTION OF PROGRESSIVE MCI. DIFFERENTIATION BETWEEN ALZHEIMER'S DISEASE AND OTHER NEURODEGENERATIVE DISEASES

Table 7 shows the sensitivity and specificity of the conventional model that classifies MCI cases into stable and

TABLE 6. Performance of the proposed method in comparison with recently published ones.

Reference, Year	Dataset (CN+MCI+AD)	CN vs AD					MCI vs AD					CN vs MCI				
		Sens	Spec	BAC	AUC	Acc	Sens	Spec	BAC	AUC	Acc	Sens	Spec	BAC	AUC	Acc
Gupta [35],2013	232+411+200	0.9524	0.9426	0.9475	-	0.9474	0.8407	0.9211	0.8809	-	0.881	0.9223	0.8145	0.8684	-	0.8635
Payan [36],2015	755 +755+755	-	-	-	-	0.9547	-	-	-	-	0.8684	-	-	-	-	0.9211
Ahmed [33],2015	251+299+347	0.804	0.882	0.843	-	0.8377	0.4902	0.7515	0.62085	-	0.6208	0.6252	0.748	0.6866	-	0.6945
Khedher [34],2015	229+401+188	0.9127	0.8511	0.8819	-	0.8849	0.8865	0.8541	0.8703	-	0.8703	0.8216	0.8162	0.8189	-	0.8189
Suk [54],2016	52+99+51	0.92	0.98	0.95	-	0.9509	0.505	0.9267	0.7159	-	0.7415	0.9389	0.5367	0.7378	-	0.8011
Korolev [41],2017	61+120+50	-	-	-	0.8	0.89	-	-		0.66	0.64	-	-	-	0.67	0.63
Cui [40],2018	223+396+192	0.9063	0.9372	0.92175	0.9695	0.9229	-	-	-	-	-	0.7727	0.6996	0.73615	0.777	0.7464
Billones [44],2017	300+300+300	0.9889	0.9778	0.9834	-	0.9833	0.9	**0.9778**	**0.9389**	-	0.9389	0.9111	0.9222	0.9167	-	0.9167
Altaf [32],2018	90+105+92	**1.0**	0.9565	0.97825	-	0.978	0.75	0.9429	0.84645	-	0.853	0.9	0.9333	0.9167	-	0.918
Lee [37],2019	229+398+192	0.9632	0.9778	0.9705	-	0.9874	-	-	-	-	-	-	-	-	-	-
Basaia [42],2019	352+763+294	0.989	0.995	0.992	-	0.992	0.836	0.883	0.8595	-	0.859	0.873	0.865	0.869	-	0.871
Fang [58],2019	101+204+93	0.9826	0.983	0.9828	-	0.9858	0.8922	0.9067	0.89945	-	0.8998	0.8633	0.9188	0.89105	-	0.8893
Liu [39],2020	119+233+97	0.866	0.908	0.887	0.925	0.889		-	-	-	-	0.795	0.698	0.7465	0.775	0.762
Wang [43],2020	315+297+221	0.987	-	-	-	0.9883	**0.9245**	-	-	-	0.9361	**0.9834**	-	-	-	**0.9842**
Proposed	287+646+369	**1.0**	**1.0**	**1.0**	**1.0**	**1.0**	0.8969	0.9428	0.9199	**0.9793**	**0.9261**	0.9756	**0.9876**	**0.9816**	**0.9957**	0.9839

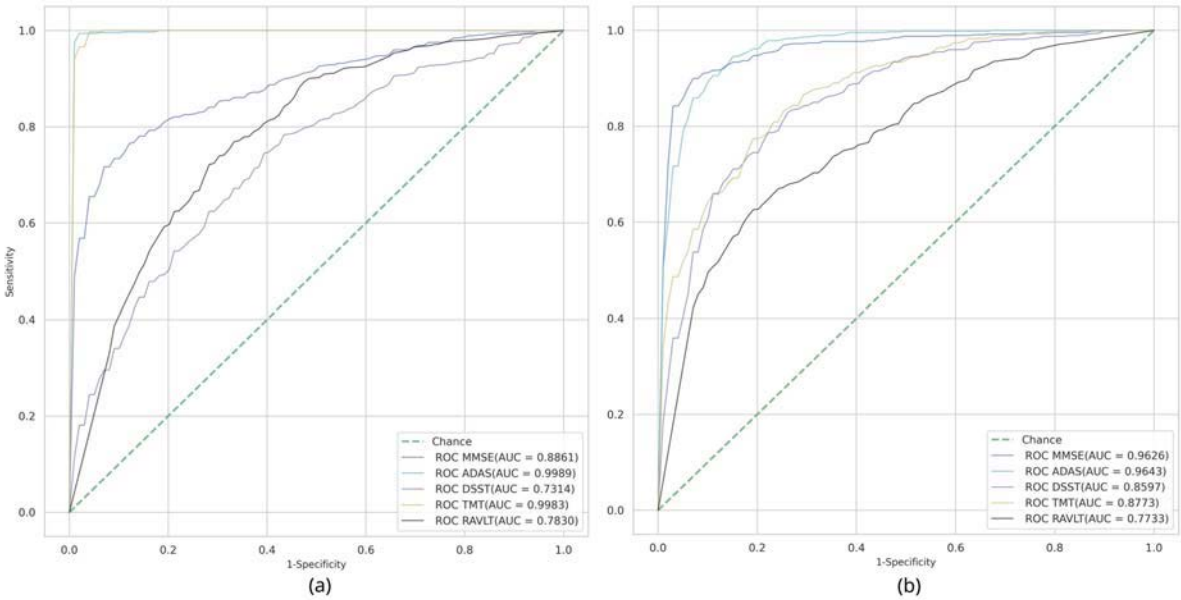

FIGURE 7. Performance of Random Forest model classifying cases into CN and MCI cohorts (a); patients with MCI and AD (b). DMNA values are the input to the model.

progressive ones. As seen from the table, there is no considerable difference in DMNA values between the groups (p=0.16÷0.21). Though the balanced accuracy of binary classification is above 80%, low specificity can be considered as a strong limitation of the models. We also identified the difference in DMNA between *demented individuals* with A+ and A– subjects (see Table 8). Only in MMSE tests the distinction in DMNA was considerable (6.27±1.82 vs 5.32±1.9; $p < 0.05$). At the same time, there was no difference between A+ and A– *patients with MCI* ($p = 0.75 - 0.98$).

IV. DISCUSSION

A. ASSOCIATION OF COGNITIVE TESTS AND STRUCTURAL DATA

In our study the structural markers of brain aging demonstrated a stronger correlation with the results in ADAS-cog than in the other tests. Other authors also justified the informative value of ADAS-cog by predicting the ADAS-cog score with a regression model from morphometric features [20], [80]. We found an obvious correlation of MMSE score with hippocampal volume ($r = 0.44, p = 7.25e-86$). This goes in line with another study that showed their close association ($r = 0.51, p < 0.001$) [49].

The results we received suggest the presence of a distinct SFA in healthy aging and ND. For instance, the proportion of WM lesions to TIV does not show a linear association with ADAS-cog score in subjects diagnosed with MCI. In contrast to this, the relationship is strong in AD patients ($r = 0.22$; $p = 2.61e - 05$). Other authors showed that WM lesions enlarged with age and with the development of dementia [29], [81]. It remains unclear why the emergence of WM lesions has a common pattern in the CN adults and patients with AD.

We reported a prominent relationship between cognitive functioning and the volumes of hippocampus, amygdala, entorhinal cortex, and middle temporal lobe. Other studies also justified the importance of the hippocampal area, amygdala, and the middle temporal lobe for intellectual activities [82]–[93].

TABLE 7. Performance of binary classification model to distinguish between stable and progressive MCI.

		DMNA			stable vs progressive MCI				
		stable MCI ($N = 114$)	progressive MCI ($N = 518$)	p	Sens	Spec	BAC	AUC	Acc
MMSE	2.19[1.15-2.94]	2.21±1.41	2.09±1.3	0.21	0.95	0.71	0.83	0.8547	0.82
ADAS	11.1[8.32-13.63]	11.16±4.02	10.82±3.79	0.16	0.96	0.75	0.855	0.8605	0.85
MMSE + ADAS					0.96	0.67	0.815	0.9475	0.81

TABLE 8. Absolute values of DMNA according to A/T/N classification system.

	Test	A-T-N-	A-T-N+	A-T+N-	A-T+N+	A+T-N-	A+T-N+	A+T+N-	A+T+N+	p-value
MCI		MCI due to other pathology ($N = 95$)				MCI due to accumulation of β amyloid ($N = 26$)				
	MMSE	2.29 ±.141				2.23 ±1.12				0.98
	ADAS	11.22 ±3.85				11.47 ±3.45				0.75
Dementia		Non-Alzheimer's disease dementia ($N = 43$)				Dementia due to Alzheimer's disease ($N = 17$)				
	MMSE	6.27±1.82				5.32 ± 1.9				**p<0.05**
	ADAS	23.87±5.42				21.17 ± 4.81				0.1

B. DEVIATION FROM THE MODEL OF NORMAL AGING

Some authors found marked correlations between the predicted and actual scores in MMSE ($r = 0.44, p =< 0.0001$) and ADAS-cog tests ($r = 0.57, p =< 0.0001$) [19], [20]. We also observed a significant linear association between the predicted and actual values in the combined group of the CN subjects, MCI, and AD patients (MMSE $r = 0.09, p = 2.28e-4$, ADAS $r = 0.05, p = 2.87e-2$, RAVLT $r = 0.11, p = 2.24e-05$, TMT $r = 0.22, p = 2.34e-18$). We recorded conflicting findings (a non-correlation) in the CN group due to distinct study design. Stonington et. al [19] trained the model on three cohorts (CN, MCI, and AD), while we fed the predictive model exceptionally with the CN cases. Other researchers managed to predict MMSE results from fMRI data accurately [18]. The calculation of cognitive scores is more precise from the radiomics data than from the images (see Table 3). The first reason for this is the noise of the 2D images averaged along distinct axes. The second reason is the relatively low number of cases used for training the deep learning model. The high-dimensional computational model needs a larger number of training samples because of the dimensionally cursed phenomena [94].

The idea of using the deviation between the model and actual values is not new for diagnostics. There is a large body of evidence that the difference between the computed and actual age - biological age gap - is a reliable marker of dementia [95]–[97]. A study suggested an association between the gap and cognitive performance. It also reported that BAG is related to worsening in performance on the DSST and TMT tests [98]. We applied the same idea to prediction of cognitive performance.

C. DISTINCTION BETWEEN HEALTHY POPULATION, PATIENTS WITH MCI AND WITH AD

Many papers reported a high accuracy of the models that classify healthy and demented subjects [32], [33], [35], [36], [39], [40], [42], [43]. All the deep learning models were trained on pre-processed MRI images of the cognitively preserved and those with cognitive deterioration. In contrast to the studies, we trained the model exclusively on CN people.

From our data, the predictive power of an SFA model depends on the complexity of the cognitive test used for its training. The accuracy is higher for the tests covering several cognitive domains (MMSE, ADAS, TMT vs information processing in DSST, memory in RAVLT). This supports the results of a study by Stonnington et. al. [19].

We report that the model classifying MCI and AD patients has the lowest accuracy ($Acc = 0.9261$). Recently different authors received the same results [32], [35], [54], [58].

A limitation of the current research is that we did not study convertible and non-convertible to AD MCI cases separately, although some researchers suggest this [42]. Advances in DL technology allowed neuroscientists to improve the classification accuracy of CN-versus-MCI and MCI-versus-AD models [43]. However, the models were biased because of the data leakage related to the late split [99]. Thus, substantial work is required to use such algorithms as a diagnostic tool.

D. DMNA AS A MARKER OF PROGRESSIVE MCI AND DIFFERENTIATION DIAGNOSTIC TOOL

From our data, DMNA cannot be recommended as a tool for predicting the conversion of MCI to dementia because of its low specificity (up to 75%). Other existing CSF markers of progressive MCI also do not ensure the necessary level of prediction: mean diffusivity (average accuracy of 77%), tau concentration (74%), volumetry data retrieved from the brain MRI (66%) [100]. There is a considerable distinction in DMNA between demented individuals with Alzheimer's continuum (A+) and those with either normal AD biomarkers or non-AD pathologic change (A–). Hence, the proposed marker can be potentially used for differentiating dementia due to AD from non-AD dementia. To find and justify a reliable threshold level, further research is required. We failed to identify a strong distinction between MCI due to the accumulation of beta-amyloid and because of other pathologies ($p > 0.05$). From our data, the biomarker is not applicable

for discriminating MCI cases by underlying pathology (AD vs non-AD).

V. CONCLUSION

- There is a strong association between the brain structure of a subject and his/her performance in cognitive tests. However, the patterns of the structure-function association differ among cognitively preserved people, patients with MCI and with dementia. For instance, the coefficient of correlation between hippocampal volume and $ADAS_{13}$ score was -0.18 in the CN cohort, -0.34 in patients with MCI, and -0.20 in the AD group. The same coefficient in $RAVLT_{immediate}$ was 0.13, 0.24, and 0.18 in the correspondent cohorts
- To work out a new marker of neurodegeneration, we predicted the cognitive status of the cognitively preserved examinee from the brain MRI data. This was an SFA model of normal aging. A big deviation from the model of normal aging suggests a high risk of accelerated cognitive decline, i.e., a high level of the error of cognitive score prediction should rise awareness of a neurodegenerative disease.
- The results in the tests reflecting global cognitive functioning - ADAS-cog and RAVLT - had the strongest association with the structural markers of brain atrophy. In line with this, the variability of the deviation from the model of normal aging in the cognitively preserved subjects, patients with MCI and dementia is most apparent in ADAS-cog and MMSE tests and less evident in the tests covering several cognitive subdomains - RAVLT, DSST, and TMT. Diagnosing dementia from DMNA values was most accurate with Random Forest classifier jointly trained on DMNA MMSE and DMNA ADAS-cog. DMNA can accurately distinguish CN subjects from MCI patients. We also achieved creditable performance in the MCI-versus-AD classification.
- There is no considerable difference in DMNA values between stable and progressive MCI cases. DMNA as a prognostic criterium of progressive MCI has strong limitation. Both the proposed and the existing markers of progressive MCI do not ensure the necessary level of prediction.
- The proposed marker can be potentially used for differentiating dementia due to AD from non-AD dementia. We identified a considerable difference in DMNA in the MMSE test between demented individuals with (A+) and (A–) according to ATN-classification (6.27 ± 1.82 vs 5.32 ± 1.9; $p < 0.05$). To find and justify a reliable threshold level, further research is required.

ACKNOWLEDGMENT

The authors would like to acknowledge the continuous support from the College of Information Technology, UAEU, for providing access to the GPU-based computational facilities such as a supercomputer DGX-1, and the second forum for women in research (QUWA): Empowering Women in Research and Innovation (UAE, Sharjah) for valuable support. Data used in preparation of this article were obtained from the Alzheimer's Disease Neuroimaging Initiative (ADNI) database (adni.loni.usc.edu). As such, the investigators within the ADNI contributed to the design and implementation of ADNI and/or provided data but did not participate in analysis or writing of this report. A complete listing of ADNI investigators can be found at:http://adni.loni.usc.edu/wp-content/uploads/how_to_apply/ADNI_Acknowledgement_List.pdf. ADNI is funded by the National Institute on Aging, the National Institute of Biomedical Imaging and Bioengineering, and through generous contributions from the following: AbbVie, Alzheimer's Association; Alzheimer's Drug Discovery Foundation; Araclon Biotech; BioClinica, Inc.; Biogen; Bristol-Myers Squibb Company; CereSpir, Inc.; Cogstate; Eisai Inc.; Elan Pharmaceuticals, Inc.; Eli Lilly and Company; EuroImmun; F. Hoffmann-La Roche Ltd and its affiliated company Genentech, Inc.; Fujirebio; GE Healthcare; IXICO Ltd.; Janssen Alzheimer Immunotherapy Research & Development, LLC.; Johnson & Johnson Pharmaceutical Research & Development LLC.; Lumosity; Lundbeck; Merck & Co., Inc.; Meso Scale Diagnostics, LLC.; NeuroRx Research; Neurotrack Technologies; Novartis Pharmaceuticals Corporation; Pfizer Inc.; Piramal Imaging; Servier; Takeda Pharmaceutical Company; and Transition Therapeutics. The Canadian Institutes of Health Research is providing funds to support ADNI clinical sites in Canada. Private sector contributions are facilitated by the Foundation for the National Institutes of Health (www.fnih.org). The grantee organization is the Northern California Institute for Research and Education, and the study is coordinated by the Alzheimer's Therapeutic Research Institute at the University of Southern California. ADNI data are disseminated by the Laboratory for Neuro Imaging at the University of Southern California.

AUTHOR CONTRIBUTIONS

All the authors contributed to the conceptual idea of the article, wrote the manuscript, and planned the experiments. Tetiana Habuza formulated the methodology of the study, conducted the experimental work. Nazar Zaki, Yauhen Statsenko, and Elfadil A. Mohamed contributed to the critical data analysis, discussion, and interpretation of the results.

ETHICAL APPROVAL

The current study is a retrospective analysis of data that were recently collected either as a standard of care or for other research purposes. This totally complies currently existing ethical policies. The original data collection procedures were done in accordance with an institutional review board, also known as an independent ethics committee. According to ADNI: "All procedures performed in studies involving human participants were in accordance with the ethical standards of the institutional and/or national research committee and with the 1964 Helsinki declaration and its later amendments or comparable ethical standards." All necessary

patient/participant consent has been obtained. Any clinical trials involved have been registered with an ICMJE-approved registry.

REFERENCES

[1] P. Thagard, *Cognitive Science*. Evanston, IL, USA: Routledge, 2013.

[2] T. J. Palmeri, B. C. Love, and B. M. Turner, "Model-based cognitive neuroscience," *J. Math. Psychol.*, vol. 76, pp. 59–64, 2017.

[3] R. D. Beer, "Dynamical approaches to cognitive science," *Trends Cognit. Sci.*, vol. 4, no. 3, pp. 91–99, Mar. 2000.

[4] R. J. Perrin, A. M. Fagan, and D. M. Holtzman, "Multimodal techniques for diagnosis and prognosis of Alzheimer's disease," *Nature*, vol. 461, pp. 916–922, Oct. 2009.

[5] *Estimation of the Global Prevalence of Dementia in 2019 and Forecasted Prevalence in 2050: An Analysis for the Global Burden of Disease Study 2019*, The Lancet Public Health, G. D. F. Collaborators, GBD, Dementia Forecasting Collaborators, 2019.

[6] Y. Statsenko, T. Habuza, D. Smetanina, G. L. Simiyu, L. Uzianbaeva, K. Neidl-Van Gorkom, N. Zaki, I. Charykova, J. Al Koteesh, T. M. Almansoori, M. Belghali, and M. Ljubisavljevic, "Brain morphometry and cognitive performance in normal brain aging: Age- and sex-related structural and functional changes," *Frontiers Aging Neurosci.*, vol. 13, p. 687, Jan. 2021.

[7] K. Furukawa, A. Ishiki, N. Tomita, Y. Onaka, H. Saito, T. Nakamichi, K. Hara, Y. Kusano, M. Ebara, Y. Arata, and M. Sakota, "Introduction and overview of the special issue 'Brain imaging and aging': The new era of neuroimaging in aging research," *Ageing Res. Rev.*, vol. 30, pp. 1–3, Sep. 2016.

[8] X.-H. Hou, L. Feng, C. Zhang, X.-P. Cao, L. Tan, and J.-T. Yu, "Models for predicting risk of dementia: A systematic review," *J. Neurol., Neurosurg. Psychiatry*, vol. 90, no. 4, pp. 373–379, Apr. 2019.

[9] M. Folstein, L. Robins, and J. Helzer, "The mini-mental state examination," *Arch. General Psychiatry*, vol. 40, no. 7, p. 812, 1983.

[10] M. Schmidt, *Rey Auditory Verbal Learning Test: A Handbook*, vol. 17. Los Angeles, CA, USA: Western Psychological Services, 1996.

[11] R. C. Mohs, "Administration and scoring manual for the Alzheimer's disease assessment scale," The Mount Sinai School Med., New York, NY, USA, 1994.

[12] D. Wechsler, *WAIS-R Manual: Wechsler Adult Intelligence Scale-Revised*. San Antonio, TX, USA: Psychological Corporation, 1981.

[13] E. Strauss, E. M. S. Sherman, and O. Spreen, *A Compendium of Neuropsychological Tests: Administration, Norms, and Commentary*. Oxford, U.K.: Oxford Univ. Press, 1998.

[14] J. C. Morris, "Clinical dementia rating: A reliable and valid diagnostic and staging measure for dementia of the Alzheimer type," *Int. Psychogeriatrics*, vol. 9, no. S1, pp. 173–176, Dec. 1997.

[15] D. Wechsler, *Wechsler memory scale-revised (WMS-R)*. Psychological Corporation, 1987.

[16] E. Pellegrini, L. Ballerini, M. D. C. V. Hernandez, F. M. Chappell, V. González-Castro, D. Anblagan, S. Danso, S. Muñoz-Maniega, D. Job, C. Pernet, G. Mair, T. J. MacGillivray, E. Trucco, and J. M. Wardlaw, "Machine learning of neuroimaging for assisted diagnosis of cognitive impairment and dementia: A systematic review," *Alzheimer's Dementia: Diagnosis, Assessment Disease Monitor.*, vol. 10, no. 1, pp. 519–535, Jan. 2018.

[17] S. Lahmiri and A. Shmuel, "Performance of machine learning methods applied to structural MRI and ADAS cognitive scores in diagnosing Alzheimer's disease," *Biomed. Signal Process. Control*, vol. 52, pp. 414–419, Jul. 2019.

[18] N. T. Duc, S. Ryu, M. N. I. Qureshi, M. Choi, K. H. Lee, and B. Lee, "3D-deep learning based automatic diagnosis of Alzheimer's disease with joint MMSE prediction using resting-state fMRI," *Neuroinformatics*, vol. 18, no. 1, pp. 71–86, Jan. 2020.

[19] C. M. Stonnington, C. Chu, S. Klöppel, C. R. Jack, J. Ashburner, and R. S. Frackowiak, "Predicting clinical scores from magnetic resonance scans in Alzheimer's disease," *NeuroImage*, vol. 51, no. 4, pp. 1405–1413, 2010.

[20] B. Lei, W. Hou, W. Zou, X. Li, C. Zhang, and T. Wang, "Longitudinal score prediction for Alzheimer's disease based on ensemble correntropy and spatial–temporal constraint," *Brain Imag. Behav.*, vol. 13, no. 1, pp. 126–137, Feb. 2019.

[21] S. Walter, C. Dufouil, A. L. Gross, R. N. Jones, D. Mungas, T. J. Filshtein, J. J. Manly, T. E. Arpawong, and M. M. Glymour, "Neuropsychological test performance and MRI markers of dementia risk," *Alzheimer Disease Associated Disorders*, vol. 33, no. 3, pp. 179–185, 2019.

[22] R. Rodríguez-Labrada, L. Velázquez-Pérez, R. Ortega-Sánchez, A. Peña-Acosta, Y. Vázquez-Mojena, N. Canales-Ochoa, J. Medrano-Montero, R. Torres-Vega, and Y. González-Zaldivar, "Insights into cognitive decline in spinocerebellar ataxia type 2: A P300 event-related brain potential study," *Cerebellum Ataxias*, vol. 6, no. 1, p. 3, Dec. 2019.

[23] C. R. Jack, D. S. Knopman, W. J. Jagust, R. C. Petersen, M. W. Weiner, P. S. Aisen, L. M. Shaw, P. Vemuri, H. J. Wiste, S. D. Weigand, T. G. Lesnick, V. S. Pankratz, M. C. Donohue, and J. Q. Trojanowski, "Tracking pathophysiological processes in Alzheimer's disease: An updated hypothetical model of dynamic biomarkers," *Lancet Neurol.*, vol. 12, no. 2, pp. 207–216, Feb. 2013.

[24] H. Matsuda, "MRI morphometry in Alzheimer's disease," *Ageing Res. Rev.*, vol. 30, pp. 17–24, Sep. 2016.

[25] M. W. Vernooij, F. B. Pizzini, R. Schmidt, M. Smits, T. A. Yousry, N. Bargallo, G. B. Frisoni, S. Haller, and F. Barkhof, "Dementia imaging in clinical practice: A European-wide survey of 193 centres and conclusions by the ESNR working group," *Neuroradiology*, vol. 61, no. 6, pp. 633–642, Jun. 2019.

[26] P. Coupé, J. V. Manjón, E. Lanuza, and G. Catheline, "Lifespan changes of the human brain in Alzheimer's disease," *Sci. Rep.*, vol. 9, no. 1, pp. 1–12, 2019.

[27] T. M. Hughes, L. H. Kuller, E. J. M. Barinas-Mitchell, R. H. Mackey, E. M. McDade, W. E. Klunk, H. J. Aizenstein, A. D. Cohen, B. E. Snitz, C. A. Mathis, S. T. DeKosky, and O. L. Lopez, "Pulse wave velocity is associated with β-amyloid deposition in the brains of very elderly adults," *Neurology*, vol. 81, no. 19, pp. 1711–1718, Nov. 2013.

[28] A. M. Pietroboni, M. Scarioni, T. Carandini, P. Basilico, M. Cadioli, G. Giulietti, A. Arighi, M. Caprioli, L. Serra, C. Sina, and C. Fenoglio, "CSF β-amyloid and white matter damage: A new perspective on Alzheimer's disease," *J. Neurol., Neurosurg. Psychiatry*, vol. 89, no. 4, pp. 352–357, 2018.

[29] K. Wei, T. Tran, K. Chu, M. T. Borzage, M. N. Braskie, M. G. Harrington, and K. S. King, "White matter hypointensities and hyperintensities have equivalent correlations with age and CSF β-amyloid in the nondemented elderly," *Brain Behav.*, vol. 9, no. 12, Dec. 2019, Art. no. e01457.

[30] M. R. Ahmed, Y. Zhang, Z. Feng, B. Lo, O. T. Inan, and H. Liao, "Neuroimaging and machine learning for dementia diagnosis: Recent advancements and future prospects," *IEEE Rev. Biomed. Eng.*, vol. 12, pp. 19–33, 2019.

[31] T. Habuza, A. N. Navaz, F. Hashim, F. Alnajjar, N. Zaki, M. A. Serhani, and Y. Statsenko, "AI applications in robotics, precision medicine, and medical image analysis: An overview and future trends," *Informat. Med. Unlocked*, vol. 2021, May 2021, Art. no. 100596.

[32] T. Altaf, S. M. Anwar, N. Gul, M. N. Majeed, and M. Majid, "Multi-class Alzheimer's disease classification using image and clinical features," *Biomed. Signal Process. Control*, vol. 43, pp. 64–74, May 2018.

[33] O. B. Ahmed, M. Mizotin, J. Benois-Pineau, M. Allard, G. Catheline, and C. B. Amar, "Alzheimer's disease diagnosis on structural MR images using circular harmonic functions descriptors on hippocampus and posterior cingulate cortex," *Computerized Med. Imag. Graph.*, vol. 44, pp. 13–25, Sep. 2015.

[34] L. Khedher, J. Ramírez, J. M. Górriz, A. Brahim, and F. Segovia, "Early diagnosis of Alzheimer's disease based on partial least squares, principal component analysis and support vector machine using segmented MRI images," *Neurocomputing*, vol. 151, pp. 139–150, Mar. 2015.

[35] A. Gupta, M. Ayhan, and A. Maida, "Natural image bases to represent neuroimaging data," in *Proc. Int. Conf. Mach. Learn.*, 2013, pp. 987–994.

[36] A. Payan and G. Montana, "Predicting Alzheimer's disease: A neuroimaging study with 3D convolutional neural networks," 2015, *arXiv:1502.02506*.

[37] B. Lee, W. Ellahi, and J. Y. Choi, "Using deep CNN with data permutation scheme for classification of Alzheimer's disease in structural magnetic resonance imaging (sMRI)," *IEICE Trans. Inf. Syst.*, vol. 102, no. 7, pp. 1384–1395, 2019.

[38] T. Habuza, N. Zaki, Y. Statsenko, F. Alnajjar, and S. Elyassami, "Predicting the diagnosis of dementia from MRI data: Added value to cognitive tests," in *Proc. ArabWIC : 7th Annu. Int. Conf. Arab Women Comput. Conjunct 2nd Forum Women Res.*, Aug. 2021, pp. 1–7.

[39] M. Liu, F. Li, H. Yan, K. Wang, Y. Ma, L. Shen, and M. Xu, "A multi-model deep convolutional neural network for automatic hippocampus segmentation and classification in Alzheimer's disease," *NeuroImage*, vol. 208, Mar. 2020, Art. no. 116459.
[40] R. Cui and M. Liu, "Hippocampus analysis by combination of 3-D DenseNet and shapes for Alzheimer's disease diagnosis," *IEEE J. Biomed. Health Informat.*, vol. 23, no. 5, pp. 2099–2107, Sep. 2019.
[41] S. Korolev, A. Safiullin, M. Belyaev, and Y. Dodonova, "Residual and plain convolutional neural networks for 3D brain MRI classification," in *Proc. IEEE 14th Int. Symp. Biomed. Imag. (ISBI)*, Apr. 2017, pp. 835–838.
[42] S. Basaia, F. Agosta, L. Wagner, E. Canu, G. Magnani, R. Santangelo, and M. Filippi, "Automated classification of Alzheimer's disease and mild cognitive impairment using a single MRI and deep neural networks," *NeuroImage: Clin.*, vol. 21, 2019, Art. no. 101645.
[43] S. Wang, H. Wang, A. C. Cheung, Y. Shen, and M. Gan, "Ensemble of 3D densely connected convolutional network for diagnosis of mild cognitive impairment and Alzheimer's disease," in *Deep Learning Application*. Singapore: Springer, 2020, pp. 53–73.
[44] C. D. Billones, O. J. L. D. Demetria, D. E. D. Hostallero, and P. C. Naval, "DemNet: A convolutional neural network for the detection of Alzheimer's disease and mild cognitive impairment," in *Proc. IEEE Region 10 Conf. (TENCON)*, Nov. 2016, pp. 3724–3727.
[45] S. A. Soliman, E.-S. A. El-Dahshan, and A.-B. M. Salem, "Deep learning 3D convolutional neural networks for predicting Alzheimer's disease (ALD)," in *New Approaches for Multidimensional Signal Processing*. Singapore: Springer, 2022, pp. 151–162.
[46] H. Qiao, L. Chen, and F. Zhu, "Ranking convolutional neural network for Alzheimer's disease mini-mental state examination prediction at multiple time-points," *Comput. Methods Programs Biomed.*, vol. 213, Jan. 2022, Art. no. 106503.
[47] Y. Gao, H. Huang, and L. Zhang, "Predicting Alzheimer's disease using 3DMgNet," 2022, *arXiv:2201.04370*.
[48] X. Liu, D. Tosun, M. W. Weiner, and N. Schuff, "Locally linear embedding (LLE) for MRI based Alzheimer's disease classification," *NeuroImage*, vol. 83, pp. 148–157, Dec. 2013.
[49] L. Sørensen, C. Igel, N. Liv Hansen, M. Osler, M. Lauritzen, E. Rostrup, and M. Nielsen, "Early detection of Alzheimer's disease using MRI hippocampal texture," *Hum. Brain Mapping*, vol. 37, no. 3, pp. 1148–1161, Mar. 2016.
[50] K. A. Ellis, A. I. Bush, D. Darby, D. De Fazio, J. Foster, P. Hudson, N. T. Lautenschlager, N. Lenzo, R. N. Martins, P. Maruff, and C. Masters, "The Australian imaging, biomarkers and lifestyle (AIBL) study of aging: Methodology and baseline characteristics of 1112 individuals recruited for a longitudinal study of Alzheimer's disease," *Int. Psychogeriatrics*, vol. 21, no. 4, pp. 672–687, Aug. 2009.
[51] M. Osler, R. Lund, M. Kriegbaum, U. Christensen, and A.-M.-N. Andersen, "Cohort profile: The metropolit 1953 Danish male birth cohort," *Int. J. Epidemiol.*, vol. 35, no. 3, pp. 541–545, Jun. 2006.
[52] F. Li, L. Tran, K. H. Thung, S. Ji, D. Shen, and J. Li, "A robust deep model for improved classification of AD/MCI patients," *IEEE J. Biomed. Health Inform.*, vol. 19, no. 5, pp. 1610–1616, Sep. 2015.
[53] E. Hosseini-Asl, R. Keynton, and A. El-Baz, "Alzheimer's disease diagnostics by adaptation of 3D convolutional network," in *Proc. IEEE Int. Conf. Image Process. (ICIP)*, Sep. 2016, pp. 126–130.
[54] H.-I. Suk, S.-W. Lee, and D. Shen, "Deep sparse multi-task learning for feature selection in Alzheimer's disease diagnosis," *Brain Struct. Function*, vol. 221, no. 5, pp. 2569–2587, 2016.
[55] X. W. Gao, R. Hui, and Z. Tian, "Classification of CT brain images based on deep learning networks," *Comput. Methods Programs Biomed.*, vol. 138, pp. 49–56, Jan. 2017.
[56] J. Zhang, M. Liu, L. An, Y. Gao, and D. Shen, "Alzheimer's disease diagnosis using landmark-based features from longitudinal structural MR images," *IEEE J. Biomed. Health Inform.*, vol. 21, no. 6, pp. 1607–1616, Nov. 2017.
[57] M. Liu, D. Cheng, K. Wang, Y. Wang, and The Alzheimer's Disease Neuroimaging Initiative, "Multi-modality cascaded convolutional neural networks for Alzheimer's disease diagnosis," *Neuroinformatics*, vol. 16, nos. 3–4, pp. 295–308, Oct. 2018.
[58] X. Fang, Z. Liu, and M. Xu, "Ensemble of deep convolutional neural networks based multi-modality images for Alzheimer's disease diagnosis," *IET Image Process.*, vol. 14, no. 2, pp. 318–326, Feb. 2020.
[59] J. Zhang, B. Zheng, A. Gao, X. Feng, D. Liang, and X. Long, "A 3D densely connected convolution neural network with connection-wise attention mechanism for Alzheimer's disease classification," *Magn. Reson. Imag.*, vol. 78, pp. 119–126, May 2021.
[60] V. Sathiyamoorthi, A. K. Ilavarasi, K. Murugeswari, S. T. Ahmed, B. A. Devi, and M. Kalipindi, "A deep convolutional neural network based computer aided diagnosis system for the prediction of Alzheimer's disease in MRI images," *Measurement*, vol. 171, Feb. 2021, Art. no. 108838.
[61] A. Qiu, L. Xu, and C. Liu, "Predicting diagnosis 4 years prior to Alzheimer's disease incident," *NeuroImage, Clin.*, vol. 34, 2022, Art. no. 102993.
[62] (2022). *ADNI1 Dataset*. [Online]. Available: https://ida.loni.usc.edu/login.jsp
[63] (2021). *MRI Acquisition in ADNI*. Accessed: Nov. 12, 2021. [Online]. Available: http://adni.loni.usc.edu/methods/mri-tool/mri-acquisition/
[64] (2021). *ADNI General Procedures Manual*. Accessed: Nov. 12, 2021. [Online]. Available: https://adni.loni.usc.edu/wp-content/uploads/2010/09/ADNI_GeneralProcedures% Manual.pdf
[65] C. R. Jack, Jr., D. A. Bennett, K. Blennow, M. C. Carrillo, B. Dunn, S. B. Haeberlein, D. M. Holtzman, W. Jagust, F. Jessen, J. Karlawish, and E. Liu, "NIA-AA research framework: Toward a biological definition of Alzheimer's disease," *Alzheimer's Dementia*, vol. 14, no. 4, pp. 535–562, 2018.
[66] J. L. Ebenau, T. Timmers, L. M. Wesselman, I. M. Verberk, S. C. Verfaillie, R. E. Slot, A. C. Van Harten, C. E. Teunissen, F. Barkhof, K. A. Van Den Bosch, and M. Van Leeuwenstijn, "ATN classification and clinical progression in subjective cognitive decline: The science project," *Neurology*, vol. 95, no. 1, pp. e46–e58, 2020.
[67] B. M. Tijms, E. A. J. Willemse, M. D. Zwan, S. D. Mulder, P. J. Visser, B. N. M. van Berckel, W. M. van der Flier, P. Scheltens, and C. E. Teunissen, "Unbiased approach to counteract upward drift in cerebrospinal fluid amyloid-β 1–42 analysis results," *Clin. Chem.*, vol. 64, no. 3, pp. 576–585, Mar. 2018.
[68] C. Mulder, N. A. Verwey, W. M. van der Flier, F. H. Bouwman, A. Kok, E. J. van Elk, P. Scheltens, and M. A. Blankenstein, "Amyloid-β(1–42), total tau, and phosphorylated tau as cerebrospinal fluid biomarkers for the diagnosis of Alzheimer disease," *Clin. Chem.*, vol. 56, no. 2, pp. 248–253, Feb. 2010.
[69] Y.-N. Ou, W. Xu, J.-Q. Li, Y. Guo, M. Cui, K.-L. Chen, Y.-Y. Huang, Q. Dong, L. Tan, and J.-T. Yu, "Fdg-pet as an independent biomarker for Alzheimer's biological diagnosis: A longitudinal study," *Alzheimer's Res. Therapy*, vol. 11, no. 1, pp. 1–11, 2019.
[70] M. Jenkinson, C. F. Beckmann, T. E. Behrens, M. W. Woolrich, and S. M. Smith, "FSL," *NeuroImage*, vol. 62, no. 2, pp. 782–790, 2012.
[71] N. J. Tustison, B. B. Avants, P. A. Cook, Y. Zheng, A. Egan, P. A. Yushkevich, and J. C. and Gee, "N4ITK: Improved N3 bias correction," *IEEE Trans. Med. Imag.*, vol. 29, no. 6, pp. 1310–1320, Jun. 2010.
[72] X. Zhu, H. I. Suk, L. Wang, S.-W. Lee, and D. Shen, "A novel relational regularization feature selection method for joint regression and classification in AD diagnosis," *Med. Image Anal.*, vol. 38, pp. 205–214, May 2017.
[73] K. Gorgolewski, C. D. Burns, C. Madison, D. Clark, Y. O. Halchenko, M. L. Waskom, and S. S. Ghosh, "Nipype: A flexible, lightweight and extensible neuroimaging data processing framework in Python," *Frontiers Neuroinform.*, vol. 5, p. 13, Aug. 2011.
[74] (2021). *Freesurfer Software Suite*. Accessed: Nov. 12, 2021. [Online]. Available: https://surfer.nmr.mgh.harvard.edu/fswiki/FreeSurferWiki
[75] (2021). *Scipy is Open-Source Software for Mathematics, Science, and Engineering*. Accessed: Nov. 12, 2021. [Online]. Available: https://docs.scipy.org/doc/scipy/reference/index.html
[76] T. Habuza, K. Khalil, N. Zaki, F. Alnajjar, and M. Gochoo, "Web-based multi-user concurrent job scheduling system on the shared computing resource objects," in *Proc. 14th Int. Conf. Innov. Inf. Technol. (IIT)*, Nov. 2020, pp. 221–226.
[77] A. Alsultan, J. J. Furin, J. Du Bois, E. van Brakel, P. Chheng, A. Venter, B. Thiel, S. A. Debanne, W. H. Boom, A. H. Diacon, and J. L. Johnson, "Population pharmacokinetics of AZD-5847 in adults with tuberculosis Abdullah Alsultan1, 2, Jennifer J. Furin3, Jeannine Du Bois4, Elana van Brakel4, Phalkun Chheng3, Amour Venter5, Bonnie Thiel3, Sara A," *Population*, vol. 61, no. 10, p. 1, 2016.
[78] E. Moradi, I. Hallikainen, T. Hänninen, and J. Tohka, "Rey's auditory verbal learning test scores can be predicted from whole brain MRI in Alzheimer's disease," *NeuroImage, Clin.*, vol. 13, pp. 415–427, Jan. 2017.

[79] M. N. Sabbagh, S. Hendrix, and J. E. Harrison, "FDA position statement 'early Alzheimer's disease: Developing drugs for treatment, guidance for industry,'" *Alzheimer's Dementia, Transl. Res. Clin. Interventions*, vol. 5, pp. 13–19, Jan. 2019.
[80] B. Jie, M. Liu, J. Liu, D. Zhang, and D. Shen, "Temporally constrained group sparse learning for longitudinal data analysis in Alzheimer's disease," *IEEE Trans. Biomed. Eng.*, vol. 64, no. 1, pp. 238–249, Jan. 2016.
[81] S. Hatashita and D. Wakebe, "Amyloid-β deposition and long-term progression in mild cognitive impairment due to Alzheimer's disease defined with amyloid PET imaging," *J. Alzheimer's Disease*, vol. 57, no. 3, pp. 765–773, Apr. 2017.
[82] H. Eichenbaum, "Hippocampus: Cognitive processes and neural representations that underlie declarative memory," *Neuron*, vol. 44, no. 1, pp. 109–120, 2004.
[83] D. Kumaran, "The human hippocampus: Cognitive maps or relational memory?" *J. Neurosci.*, vol. 25, no. 31, pp. 7254–7259, Aug. 2005.
[84] R. D. Rubin, P. D. Watson, M. C. Duff, and N. J. Cohen, "The role of the hippocampus in flexible cognition and social behavior," *Frontiers Hum. Neurosci.*, vol. 8, p. 742, Sep. 2014.
[85] I. Driscoll, "The aging hippocampus: Cognitive, biochemical and structural findings," *Cerebral Cortex*, vol. 13, no. 12, pp. 1344–1351, Dec. 2003.
[86] J. Lisman, G. Buzsáki, H. Eichenbaum, L. Nadel, C. Ranganath, and A. D. Redish, "Viewpoints: How the hippocampus contributes to memory, navigation and cognition," *Nature Neurosci.*, vol. 20, no. 11, pp. 1434–1447, Nov. 2017.
[87] A. Bechara, H. Damasio, and A. R. Damasio, "Role of the amygdala in decision-making," *Ann. New York Acad. Sci.*, vol. 985, no. 1, pp. 356–369, Jan. 2006.
[88] S. P. Poulin, R. Dautoff, J. C., Morris, L. F. Barrett, and B. C. Dickerson, "Amygdala atrophy is prominent in early Alzheimer's disease and relates to symptom severity," *Psychiatry Res., Neuroimag.*, vol. 194, no. 1, pp. 7–13, 2011.
[89] K. M. Gothard, "Multidimensional processing in the amygdala," *Nature Rev. Neurosci.*, vol. 21, no. 10, pp. 565–575, Oct. 2020.
[90] J. M. G. van Bergen, X. Li, F. C. Quevenco, A. F. Gietl, V. Treyer, S. E. Leh, R. Meyer, A. Buck, P. A. Kaufmann, R. M. Nitsch, P. C. M. van Zijl, C. Hock, and P. G. Unschuld, "Low cortical iron and high entorhinal cortex volume promote cognitive functioning in the oldest-old," *Neurobiol. Aging*, vol. 64, pp. 68–75, Apr. 2018.
[91] C. Pennanen, M. Kivipelto, S. Tuomainen, P. Hartikainen, T. Hänninen, M. P. Laakso, M. Hallikainen, M. Vanhanen, A. Nissinen, E. L. Helkala, and P.Vainio, "Hippocampus and entorhinal cortex in mild cognitive impairment and early AD," *Neurobiol. Aging*, vol. 25, no. 3, pp. 303–310, Mar. 2004.
[92] L. Velayudhan, P. Proitsi, E. Westman, J.-S. Muehlboeck, P. Mecocci, B. Vellas, M. Tsolaki, I. Kłoszewska, H. Soininen, C. Spenger, A. Hodges, J. Powell, S. Lovestone, A. Simmons, and A. consortium, "Entorhinal cortex thickness predicts cognitive decline in Alzheimer's disease," *J. Alzheimer's Disease*, vol. 33, no. 3, pp. 755–766, Jan. 2013.
[93] E. Coutureau and G. Di Scala, "Entorhinal cortex and cognition," *Prog. Neuro-Psychopharmacol. Biol. Psychiatry*, vol. 33, no. 5, pp. 753–761, Aug. 2009.
[94] J. Berner, P. Grohs, and A. Jentzen, "Analysis of the generalization error: Empirical risk minimization over deep artificial neural networks overcomes the curse of dimensionality in the numerical approximation of black-scholes partial differential equations," *SIAM J. Math. Data Sci.*, vol. 2, no. 3, pp. 631–657, Jan. 2020.
[95] J. H. Cole, R. P. Poudel, D. Tsagkrasoulis, M. W. Caan, C. Steves, T. D. Spector, and G. Montana, "Predicting brain age with deep learning from raw imaging data results in a reliable and heritable biomarker," *NeuroImage*, vol. 163, pp. 115–124, Dec. 2017.
[96] C. Bermudez, A. J. Plassard, S. Chaganti, Y. Huo, K. S. Aboud, L. E. Cutting, S. M. Resnick, and B. A. Landman, "Anatomical context improves deep learning on the brain age estimation task," *Magn. Reson. Imag.*, vol. 62, pp. 70–77, Oct. 2019.
[97] X. Feng, Z. C. Lipton, J. Yang, S. A. Small, and F. A. Provenzano, "Estimating brain age based on a uniform healthy population with deep learning and structural magnetic resonance imaging," *Neurobiol. Aging*, vol. 91, pp. 15–25, Jul. 2020.
[98] B. A. Jonsson, G. Bjornsdottir, T. E. Thorgeirsson, L. M. Ellingsen, G. B. Walters, D. F. Gudbjartsson, H. Stefansson, K. Stefansson, and M. O. Ulfarsson, "Brain age prediction using deep learning uncovers associated sequence variants," *Nature Commun.*, vol. 10, no. 1, pp. 1–10, Dec. 2019.
[99] J. Wen, E. Thibeau-Sutre, M. Diaz-Melo, J. Samper-González, A. Routier, S. Bottani, D. Dormont, S. Durrleman, N. Burgos, and O. Colliot, "Convolutional neural networks for classification of Alzheimer's disease: Overview and reproducible evaluation," *Med. Image Anal.*, vol. 63, Jul. 2020, Art. no. 101694.
[100] G. Douaud, R. A. L. Menke, A. Gass, A. U. Monsch, A. Rao, B. Whitcher, G. Zamboni, P. M. Matthews, M. Sollberger, and S. Smith, "Brain microstructure reveals early abnormalities more than two years prior to clinical progression from mild cognitive impairment to Alzheimer's disease," *J. Neurosci.*, vol. 33, no. 5, pp. 2147–2155, Jan. 2013.

TETIANA HABUZA received the bachelor's degree in applied mathematics and the master's degree in informatics from Yuriy Fedkovych Chernivtsi National University, Chernivtsi, Ukraine, in 2004 and 2005, respectively. She is currently pursuing the Ph.D. degree in computer science with United Arab Emirates University (UAEU). In 2018, having a strong interest in data science and research, she returned to academia and joined UAEU. Currently, she mainly focuses on using advanced machine learning techniques to automatically detect valuable biomarkers from medical images. Her research interests include artificial intelligence, machine learning (deep learning), bioinformatics, and control theory.

NAZAR ZAKI is a Professor of computer science with the Department of Computer Science and Software Engineering, United Arab Emirates University (UAEU). He is the Founder and the Director of the Big Data Analytics Center, UAEU. He mainly focuses on developing intelligent algorithms to solve problems in domains, such as education, biology, and healthcare. He has published more than 120 scientific results in reputable journals and conferences. His research interests include data mining and machine learning. He received several scholarship awards, such as the College Recognition Award for Excellence in Scholarship and the Chancellor's Annotation Award in technology. He is also a frequent recipient of certificates of achievement for publishing in top journals and bringing recognition to the UAEU.

ELFADIL A. MOHAMED has received the Ph.D. degree in computer science from Universiti Teknologi Malaysia, Malaysia, in 2002. He is currently working as an Assistant Professor with the College of Engineering and Information Technology, Ajman University, United Arab Emirates. He has published several scientific results in reputable journals and leading conferences. His research interests include data analysis, data mining, and databases.

YAUHEN STATSENKO is an Associate Professor with the Radiology Department, College of Medicine and Health Sciences, UAEU. He has published more than 100 scientific results in reputable journals and conferences. His research interests include mathematical modeling of aging, regeneration process, early diagnostics methods of maladjustment diseases (acupuncture diagnosing, psychophysiological testing), and prediction and treatment sport overtraining syndrome (decrease in adaptation reserve and athletic performance).